Phonon anomalies and structural stability in the $R_{2-x}Ce_xCuO_4$ system (R=Gd,Sm,Nd,Pr)

E. T. Heyen, R. Liu,* and M. Cardona
Max-Planck-Institut für Festkörperforschung, Heisenbergstrasse 1, D-7000 Stuttgart 80, Federal Republic of Germany

S. Piñol,† R. J. Melville, and D. McK. Paul
Department of Physics, University of Warwick, Coventry, Great Britain

E. Morán and M. A. Alario-Franco
Departamento de Química Inorgánica, Facultad de Ciencias Químicas, Universidad Complutense, 28040 Madrid, Spain

(Received 3 August 1990)

We present a comprehensive analysis of Raman spectra in the $R_{2-x}Ce_xCuO_4$ system (R=Gd,Sm,Nd,Pr) as a function of doping, temperature, rare-earth atomic radius, and Raman resonance conditions. Phonon frequencies as well as their temperature dependences behave anomalously for R=Pr: the B_{1g} phonon, for instance, softens by as much as 11 cm^{-1} when the crystal is cooled from room temperature to 10 K, while it hardens by 11 cm^{-1} for R=Nd. These observations are attributed to the fact that Pr, as the largest rare-earth atom that can give rise to the T' structure, is already close to the T' stability limit, yielding large phonon anharmonicities in this compound. The dependence of the phonon frequencies on doping is strong only for the oxygen E_g mode, which can thus be used for sample characterization. We also present and discuss phonon resonance profiles for $Nd_{1.85}Ce_{0.15}CuO_4$ and Nd_2CuO_4, which yield electronic structural information that should be compared with future calculations of the resonance profiles. Finally, we also discuss the origin of an additional large A_{1g}-symmetry peak that shows a dramatic, rare-earth-dependent resonance behavior and give a possible explanation on the grounds of a partial $T' \rightarrow T$ transition. We always observe several well-defined, unexpected vibrational peaks that seem to be intrinsic to the $R_{2-x}Ce_xCuO_4$ system, indicating crystal distortions that have not been conclusively identified by x-ray- or neutron-diffraction experiments so far.

I. INTRODUCTION

In the 2:1:4 compound system R_2CuO_4 (R= rare earth or La), three distinctly different structures have been observed so far, labeled T, T', and T^*. Most materials can become superconductors if they are doped with Ba, Sr (R= La; T structure)[1] or with Ce or Th (R=Pr, Nd, Sm, Eu; T' structure).[2,3] The T^* structure, which consists of alternating layers of T and T' structure, is observed for the alloy systems $R_{2-x}(Ce,Sr)_xCuO_4$ or $(La,R)_{2-x}Ce_xCuO_4$.[2]

The T and T' structures are both approximately body-centered tetragonal ($I4/mmm$). They differ[4] in that the out-of-plane (apical) O(2) atom is moved from the C_{4v} site symmetry position between La and Cu in the T structure to a position with D_{2d} site symmetry in the T' structure (Fig. 1). It was pointed out by Xue *et al.*[5] that this transition is driven by the radius of the rare-earth atom[6] which decreases from La to Pr, Nd, Sm, and Gd. The La—O(2) bonds are already strongly under tension, so that the smaller rare earths with higher atomic numbers cannot constitute the T structure, but rather prefer the T' structure where the R—O(2) bonds are under compression for R=Pr, and approximately normal for R=Gd. In this argument (which is important for the interpretation of phonon anomalies) the different coordination numbers have to be taken into account.[5] Most interesting, this structural transition is also accompanied by the "transition" from p-type- to n-type-doped superconductors. In the T structure, that tension partially relaxes by an orthorhombic distortion of the CuO_6 octahedra. A similar phenomenon has not been observed in the T' structure but, as we will see, the unusual bond lengths lead to unexpected Raman features.

Previous Raman investigations of $Nd_{2-x}Ce_xCuO_4$ (Refs. 7–11) and Pr_2CuO_4,[12] as well as some of the infrared reflectivity measurements,[13,14,10] focused on the symmetry determination and the assignment of the $A_{1g}+B_{1g}+2E_g$ Raman-active and $3A_{2u}+4E_u$ infrared-active phonons. Such assignments were confirmed with the help of lattice-dynamical calculations.[10,15] Nd_2CuO_4, for example, exhibits three Raman-allowed phonons:[7] The Nd A_{1g} mode near 230 cm^{-1} (at 30 K), the O(2) B_{1g} phonon near 344 cm^{-1}, and the E_g symmetry motion of the O(2)

atoms parallel to the planes near 494 cm^{-1}. For unknown reasons the E_g mode of Nd is not observed. According to the lattice-dynamical calculations[10] it is expected to lie near 160 cm^{-1}.

In Nd_2CuO_4 several other peaks have been observed with the incident light polarized parallel to the planes[7] but no explanation has been given so far, while only in Ce-doped Nd-2:1:4 samples a strong feature near 580 cm^{-1} was reported.[8,9,11] Heyen and co-workers[9,10] and independently Orera *et al.*[11] found that this peak is mainly zz-polarized and showed that it is resonantly enhanced for higher-energy excitation. They both speculated that the highest infrared-active A_{2u} phonon might become Raman active due to the disorder induced by Ce doping. The mechanism that leads to a very high intensity, even for relatively low doping, remained an open question particularly since Sugai found this peak also in undoped Pr_2CuO_4.[12]

We prepared ceramic samples by a solid-state reaction in nonstoichiometric mixtures of Nd_2O_3, CeO_2, and CuO. The powders were then pressed and fired for 24 h under 1 atm of oxygen at 1150 °C, and finally annealed under argon at 900 °C for 12 h. Details are presented elsewhere.[16]

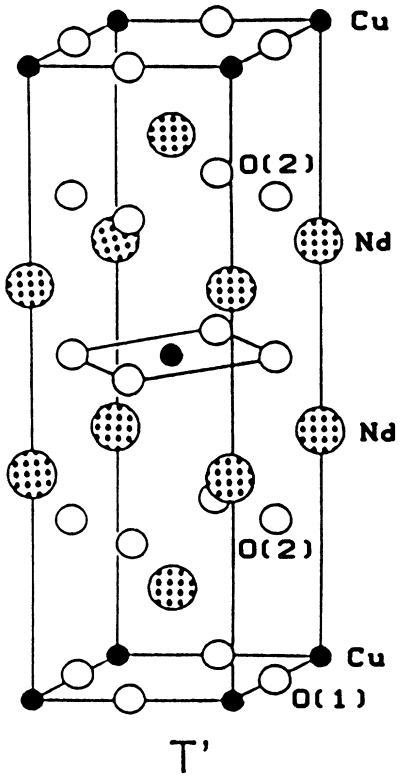

FIG. 1. T' crystal structure of Nd_2CuO_4. Shaded, solid, and open circles denote rare-earth, copper, and oxygen atoms, respectively. (Taken from Ref. 2).

We obtained single crystals with Ce contents from x=0 to 0.15 from a stoichiometric mixture of the starting materials which was heated at a rate of 500 °C/h up to 1250 °C, left for 2 h at this temperature, and then slowly cooled to 800 °C. Finally, the crucibles were cooled to room temperature by quenching them in air. The crystals which were mechanically separated from the crucible were annealed at 950 °C for 12 h under argon atmosphere.[17] They had a size of 2×2×0.05 mm^3 and mirrorlike, smooth surfaces. According to x-ray measurements, they were single phase and the Ce-doped materials (x=0.15) showed a sharp magnetic susceptibility transition at T_c=23 K.

This paper is structured as follows: In Sec. II we discuss the rare-earth dependence of the phonon frequencies and report that Pr_2CuO_4 behaves anomalously since the Pr atomic radius is almost too large to make the T' structure, so that the O(2)-atom position becomes nearly unstable. In Sec. III we show that the temperature dependence is regular for R=Gd and Sm, but anomalous for Nd and Pr, where the stability region is approached. Possibly due to strong anharmonicity, the O(2) B_{1g} phonon for R=Pr softens when the sample is cooled. We also describe the temperature dependence of the Raman intensities.

In Sec. IV we present stoichiometry-dependent Raman spectra and show that the O(2) E_g frequency might be used for Ce-content calibration purposes. No difference was observed between as-prepared and Ar-annealed samples. In Sec. V we discuss the resonance behavior of the Raman modes and compare it for different rare earths. In particular, we find that the elusive 580-cm^{-1} peak shows a different, though always dramatic, resonance behavior for varying rare earths.

Finally, in Sec. VI we summarize the properties of the 580-cm^{-1} mode and present a mechanism that could possibly explain the surprising high intensity of the 580-cm^{-1} mode.

II. RARE-EARTH DEPENDENCE

Figures 2–4 show the Raman spectra of $R_{1.85}Ce_{0.15}CuO_4$ (R=Pr,Nd,Sm,Gd) single crystals obtained in the $x(zz)\bar{x}$, $z(xx)\bar{z}$, and $x(yz)\bar{x}$ polarization configurations. We use the Porto notation $i(jk)l$, where i, l denote the direction and j, k the polarizations of incident and scattered light, respectively. It has been shown before[8–11] that the A_{1g} peak near 220 cm^{-1}, which is mostly zz polarized, corresponds exclusively (since group theory predicts only one A_{1g} mode) to the even symmetry motion of the rare-earth atoms in the z direction. Similarly the B_{1g} phonon near 320 cm^{-1} (Fig. 3), which appears also in $z(x+y,x-y)\bar{z}$ configuration (not shown here) and the E_g symmetry modes near 470 cm^{-1} (Fig. 4) belong to the z- and x/y-directed motion of the O(2) atom, respectively. The fourth mode, near 580 cm^{-1}, does not belong to any of the regular Raman phonons expected from the symmetry analysis. Since it exhibits

TABLE I. Phonon frequencies in cm^{-1} observed in $R_{1.85}Ce_{0.15}CuO_4$ single crystals at room temperature.

Rare earth	Phonon frequency (cm^{-1}) $R\ A_{1g}$	O(2) B_{1g}	O(2) E_g	A_{1g}^*
Gd	219	347	492	596
Sm	220	332	485	586
Nd	223	327	476	581
Pr	224	298	456	579

perfect A_{1g}-symmetry selection rules,[9,11] we call it "the A_{1g}^* mode." Its possible origin will be discussed in Sec. VI. The observed phonon frequencies are summarized in Table I.

For all rare earths the Raman spectra look very similar, with remarkable differences in some of the intensities (intensities for different rare earths can only be compared approximately due to different crystal shapes and surface qualities). It seems to be clear, however, that the relative strength of the A_{1g}^* mode to the other modes varies substantially. Also the Nd-2:1:4 E_g mode is particularly strong while the corresponding Pr-2:1:4 E_g mode is very weak (Fig. 4). These points will be discussed further in Sec. V. According to the x-ray-diffraction analysis, only the Gd-2:1:4 crystal exhibited a small orthorhombic

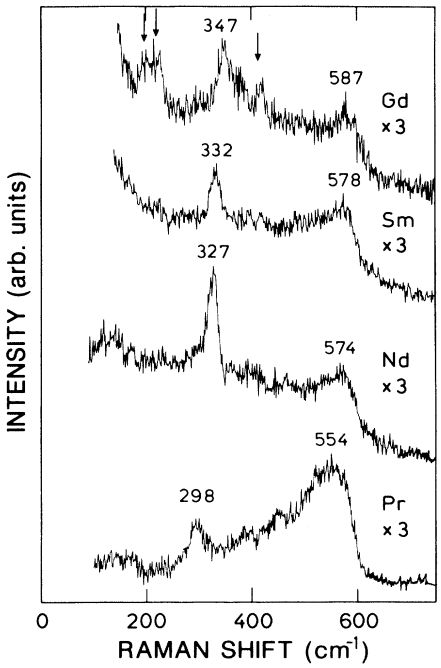

FIG. 3. Raman spectra of $R_{1.85}Ce_{0.15}CuO_4$ single crystals (R=Pr,Nd,Sm,Gd) measured at room temperature under $z(xx)\bar{z}$ polarization geometry, yielding A_{1g} and B_{1g} phonons. All spectra have been magnified by a factor of 3 with respect to Fig. 2. Peaks that are probably induced by an orthorhombic distortion in Gd-2:1:4 are marked by arrows.

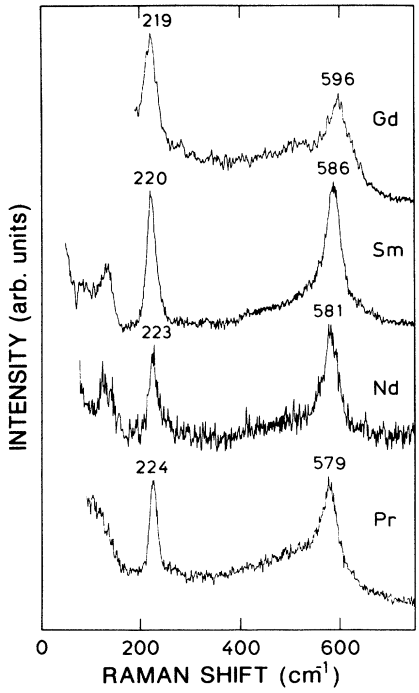

FIG. 2. Raman spectra of $R_{1.85}Ce_{0.15}CuO_4$ single crystals (R=Pr,Nd,Sm,Gd) measured at room temperature under $x(zz)\bar{x}$ polarization geometry, yielding A_{1g} phonons.

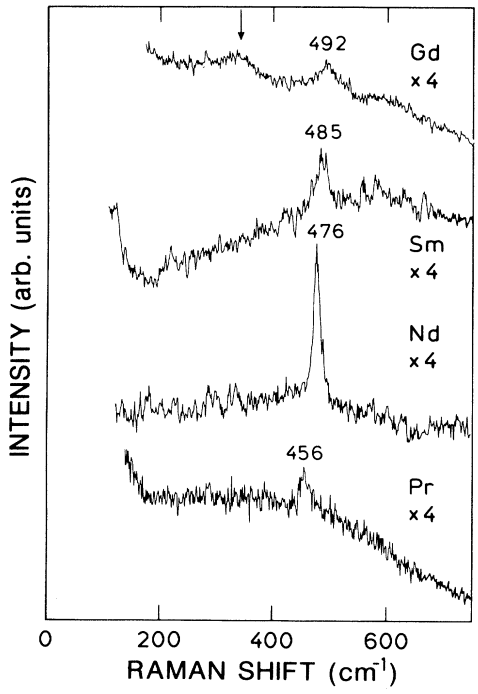

FIG. 4. Raman spectra of $R_{1.85}Ce_{0.15}CuO_4$ single crystals (R=Pr,Nd,Sm,Gd) measured at room temperature under $x(yz)\bar{x}$ polarization geometry, yielding E_g phonons. The spectra have been magnified by a factor of 4 with respect to Fig. 2.

distortion leading to the observation of additional peaks near 200 and 420 cm^{-1} (arrows in Fig. 3). We also often observed a peak near 130 cm^{-1} in the $x(zz)\bar{x}$ spectra (Fig. 2). Since its intensity was sample dependent we ignore it in this paper.

Figure 5 shows the dependence of the four strongest modes on the rare-earth radius (taken from Ref. 7). The A_{1g} rare-earth frequencies were multiplied by $\sqrt{m_R/m_{Nd}}$ to correct for trivial mass dependences. Corresponding to the known continuous increase in lattice dimensions[18] (a and c increase from Gd-2:1:4 to Pr-2:1:4 by 1.6% and 3.4%, respectively) with increasing rare-earth radii the A_{1g}- and A_{1g}^*-mode energies decrease continuously, whereas the O(2) B_{1g} and E_g modes both have an anomalously low frequency for R=Pr. We should mention here that the only free internal unit cell parameter in the T' structure, the ratio z of the vertical rare-earth–copper distance to the lattice constant c, is within 2×10^{-3} independent of rare earth, temperature, and doping[19,20] and thus cannot account for any of the effects reported in this paper.

The observed anomaly can be qualitatively understood on the basis of the paper by Xue *et al.*[5] For Nd-2:1:4 the R—O(2) bonds are already strongly compressed and for Pr-2:1:4 the compressibility limit is almost reached. With the next-largest rare-earth-like atom La, the 2:1:4 compound does not have the T' structure but rather the T structure, with the only difference in the O(2) atomic position. We can thus conclude that the potential acting on the O(2) atom becomes flatter and more anharmonic when we approach the T'-structural limit which would exist for a "rare-earth radius between Pr and La." With increasing rare-earth radii we thus expect strongly decreasing O(2) phonon frequencies, which is what we observe.

III. TEMPERATURE DEPENDENCE

The temperature dependence of the Nd-2:1:4 phonon frequencies is displayed in Fig. 6. It was shown in Ref. 20 that the lattice parameters a and c shrink by 0.19% and 0.24%, respectively, when the sample is cooled from room temperature to 10 K. If we compare this with their change when going from Gd-2:1:4 to Pr-2:1:4, the corresponding contribution to the temperature dependence of the phonon frequencies should not exceed ≈0.8% (thermal expansion effect). We see in Fig. 6 that the A_{1g}, E_g, and A_{1g}^* modes harden in agreement with this rough estimate, whereas the B_{1g} mode hardens by as much as 11 cm^{-1}, i.e., 3.4%.

The temperature dependence of phonon frequencies in the normal state of high-temperature superconductors has not yet been systematically investigated. In $YBa_2Cu_3O_{7-\delta}$, the phonons just show a regular hardening when the sample is cooled ("regular" in the sense indicated above), while other materials show a significantly stronger hardening.[21] An additional contribution to the frequency shift with temperature is produced by the de-

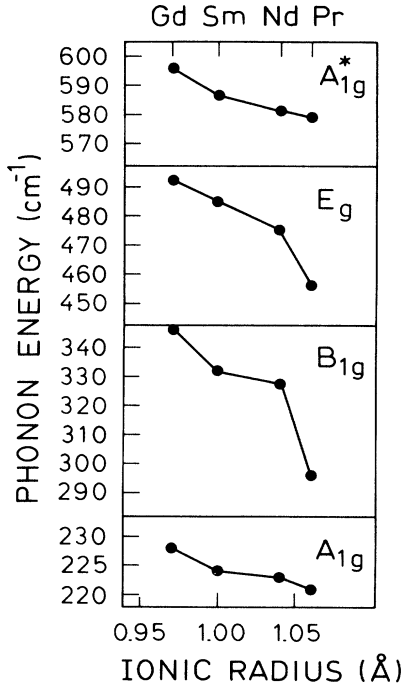

FIG. 5. Dependence of the observed phonon frequencies on rare-earth atomic radii. The rare-earth A_{1g} phonon frequencies were multiplied by $\sqrt{m_R/m_{Nd}}$ to eliminate the trivial dependence on atomic mass.

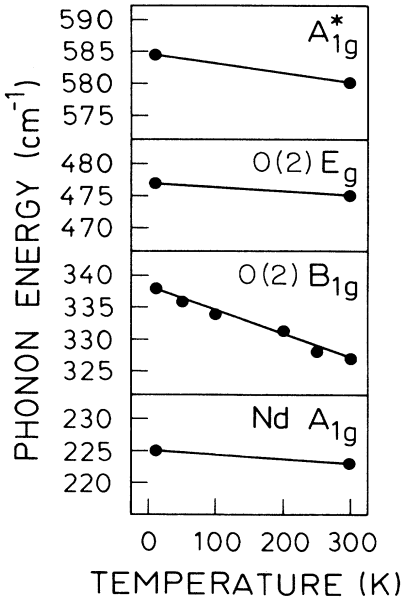

FIG. 6. Temperature dependence of the observed phonons in $Nd_{1.85}Ce_{0.15}CuO_4$.

cay of the Raman phonon into two others under energy and momentum conservation, i.e., $\omega_0 = \omega_1 + \omega_2$, $\mathbf{k}_1 + \mathbf{k}_2 = 0$. According to standard perturbation theory,[22] this "anharmonic" decay channel leads to a renormalization of phonon frequencies (self-energy effect) that is temperature dependent through the statistical factor of the ω_1 and ω_2 phonons. This may lead to hardening or softening depending on whether the "restricted two-phonon density of states $\tilde{D}(\omega)$" (integrated over all decay possibilities with $\omega = \omega_1 + \omega_2$ and $0 = \mathbf{k}_1 + \mathbf{k}_2$) peaks at an energy that is higher or lower than the phonon frequency. Actually, hardenings are usually observed (as in the case of Nd-2:1:4). It should be possible to obtain $\tilde{D}(\omega)$ from lattice-dynamical calculations and thus elucidate why only the B_{1g} mode and not the other phonons show an anomalous behavior.

This effect becomes even more dramatic if the temperature dependences of the B_{1g} phonons in the other R-2:1:4 compounds are considered (Fig. 7). (All other phonons behave "regularly.") First we notice in the third and fourth panels of Fig. 7 that the anomalous temperature behavior does not depend on the Ce content, i.e., on the carrier density. We see that with increasing rare-earth radius the slope $d\omega/dT$ becomes more negative and for Pr-2:1:4 flips its sign, yielding a large (and rarely observed) positive slope.

This is not only an indication of a highly anharmonic force field in which the O(2) atom moves for Nd-2:1:4 and Pr-2:1:4, but, in the picture of anharmonic decay into two phonons, it means that a peak in $\tilde{D}(\omega)$ has scanned across $\omega_{B_{1g}}$, from higher to lower frequencies, when the rare-earth radius is increased. Although it was demonstrated in Sec. II that the O(2) E_g phonon also behaves anomalously, it shows always a regular temperature dependence, probably because there is no sharp peak in $\tilde{D}(\omega)$ in the vicinity of its energy.

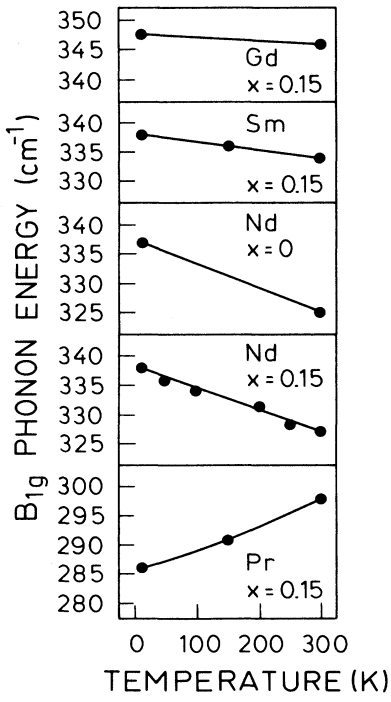

FIG. 7. Temperature dependence of the B_{1g} phonon in $R_{2-x}Ce_xCuO_4$ for various rare earths.

No anomaly in the Raman spectra was observed at the critical temperature. Since T_c is only 25% of that in $YBa_2Cu_3O_7$ we expect a superconducting gap near $2\Delta \leq 70$ cm^{-1}, i.e., in a frequency region that is difficult to measure with the spectrometer used. Phonon shifts, etc., can only occur when the phonon frequency is close to 2Δ. Since there are no Raman-active phonons at such low energies, no phonon anomalies are expected.

IV. DOPING DEPENDENCE

In the $R_{2-x}Ce_xCuO_4$ system, the trivalent rare-earth atoms can be replaced by the smaller Ce^{4+} ions with a solubility limit near x=0.20, leading to a decrease in the lattice parameter c by 0.9% and a slight increase in a by 0.25%,[23] accompanied by a ~0.2% increase in R—O(2) bond length[5] while the free parameter z (defined above) remains practically constant.[19] Lightfoot *et al.*[24] recently demonstrated by neutron scattering that $Nd_{2-x}Ce_xCuO_4$ is single phase for x=0 and 0.16 only. For other Ce contents their elastic-scattering patterns could be described by a mixture of two similar structures with slightly different lattice parameters. Unfortunately, they were not able to resolve the difference between the two phases in detail, so we cannot estimate the corresponding effect on the Raman spectra.

The dependence of Raman frequencies on Ce doping for R=Nd is plotted in Fig. 8. The z-directed A_{1g} and B_{1g} vibrational frequencies increase slightly, in agreement with the decreasing lattice parameter c, while the in-plane O(2) E_g phonon frequency decreases substantially (by 10 cm^{-1}). Again, the latter effect cannot merely be explained by the small change in lattice parameters, it is most likely due to the changes in the electronic structure induced by doping, i.e., to interaction between the E_g phonons and the added free carriers. Frozen phonon calculations[25] for varying doping could clarify this problem. This frequency variation is so large that it could be used for the determination of Ce content. Unfortunately, this approach cannot be successfully used if built-in strains are sample dependent: Our ceramic samples always show higher phonon frequencies than the single crystals (Fig. 8). We should stress at this point that in our samples the Raman spectra did not change upon annealing in argon or oxygen.

In Fig. 9, we show Raman spectra of a Nd_2CuO_4 single crystal at 10 K which are rather similar to those published by Sugai, Kobayashi, and Akimitsu.[7] We first note that the strong, zz-polarized peak near 580 cm^{-1} has completely disappeared, hence the $x(zz)\bar{x}$ and $x(zy)\bar{x}$

spectra just show the two allowed Nd A_{1g} and O(2) E_g phonons, with the Nd A_{1g} peak much narrower and higher than in Ce-doped crystals. This latter effect must be related to the perturbation of the translational symmetry of the lattice which relaxes the k-conservation selection rule.

In constrast to the Ce-doped crystals the Nd A_{1g} phonon also has a strong xx component. In addition to the O(2) B_{1g} phonon, other peaks are observed in $x*$ polarization, of which those at 203 and 589 cm^{-1} are of tetragonal B_{1g} and B_{2g} symmetry, respectively. The well-defined symmetry suggests that these features are not due to impurities but rather intrinsic. Here, as also in all low-temperature measurements on Ce-doped samples, we find that the E_g phonon is also observed in the forbidden $z(xx)\bar{z}$ polarization.

Many, partly contradictory reports on superlattice modulations,[26] in-plane oxygen vacancies, vacancy ordering,[27] and two-phase behavior[24] have been published so far. Some of these phenomena could explain the observed additional peaks, as well as the strange 580-cm^{-1} one in Ce-doped Nd-2:1:4. Since the detailed 2:1:4 structure is not known so far an assignment of the observed peaks must remain speculative. We just mention that the fact that the B_{1g} symmetry mode at 203 cm^{-1} disappears completely for T=295 K indicates a reversible ordering process at low temperatures. The B_{2g}-polarized 589-cm^{-1} mode might belong to the highest infrared-active E_u phonon corresponding to an in-plane Cu-O stretching.[10] According to its polarization behavior (seen only in xy, but not in zz polarization), it clearly has a different origin than the 581-cm^{-1} mode in Ce-doped Nd-2:1:4 (mostly zz polarized). Finally, we mention that no regular Nd_2CuO_4 phonon[10] has a frequency as high as 639 or 673 cm^{-1} (Fig. 9). Thus these peaks probably belong to local modes of displaced oxygen atoms. They could also be due to Raman scattering by two phonons.

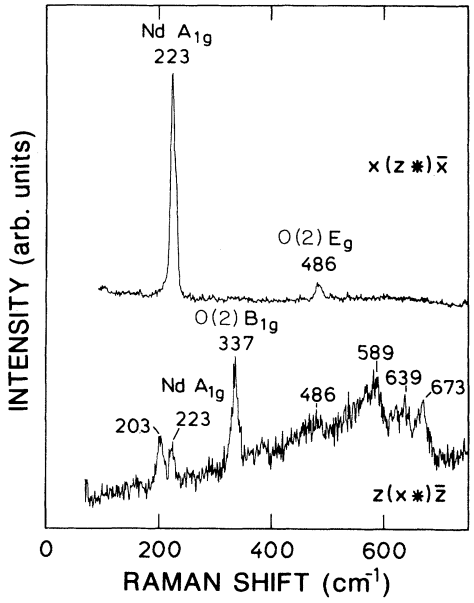

FIG. 9. Raman spectra of Nd_2CuO_4 at 10 K in $x(z*)\bar{x}$ and $z(x*)\bar{z}$ polarization, i.e., with polarized incident light and no analyzer used.

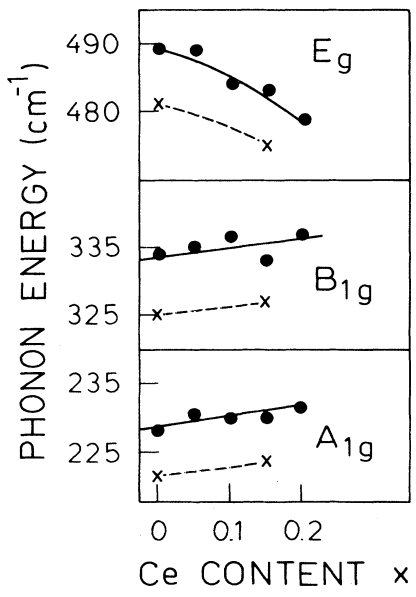

FIG. 8. Dependence of the frequencies of the three Raman-allowed phonons on Ce content in $Nd_{2-x}Ce_xCuO_4$ for ceramic samples (dots, solid lines) and single crystals (crosses, dashed lines).

V. RESONANCE RAMAN SCATTERING

Resonant Raman Scattering spectroscopy (RRS) is the measurement of the Raman intensity of a certain phonon as a function of laser energy. If the electronic resonances are broader than the phonon energy, the Raman efficiency S is given by[28]

$$S(\omega) = \frac{V}{(4\pi)^2}\left(\frac{\omega}{c}\right)^4 \left|\frac{\partial \epsilon_{is}(\omega)}{\partial q}\right|^2 , \quad (1)$$

where i and s are the polarization directions of incident and scattered light, ω is the laser angular frequency, c the velocity of light, $\epsilon_{is}(\omega)$ a component of the dielectric tensor, and q the normal coordinate of the considered phonon. RRS thus probes the variation of the dielectric function induced by a static phonon displacement (frozen phonon). It yields not only information about the dielectric function but also about its dependence on atomic positions, i.e., the electron-phonon coupling constants or deformation potentials. It has recently been shown[29] that standard LMTO (linear muffin-tin orbital) theory in

the local-density approximation (LDA) is able to describe well the dielectric function and the RRS in $YBa_2Cu_3O_7$, yielding a wealth of band-structural information. When we compare the measured intensities with those of BaF_2 and correct for absorption, reflection, and refraction effects, one can directly obtain $S(\omega)$. Since sufficient information about the dielectric tensor in $Nd_{2-x}Ce_xCuO_4$ is not available we took for the dielectric corrections just a constant, reasonable value based on the $YBa_2Cu_3O_7$ results[29] (absorption coefficient $\alpha = 1.4 \times 10^5$ cm^{-1}, reflectivity R=0.134, index of refraction n=1.94).

Figure 10 shows our results for the $Nd_{1.85}Ce_{0.15}CuO_4$ single crystal. They could be directly compared with results from band-structure calculations in order to check the validity of the latter. First, we note the dramatic increase of the A_{1g}^* mode towards the ultraviolet region, by a factor of more than 10. This observation should be important for the assignment of this feature.

We also see that the zz component of the Nd A_{1g} phonon continuously decreases when going to higher energies. The O(2) E_g phonon behaves similarly while the O(2) B_{1g} intensity is rather constant. In the blue region, the A_{1g}^* mode is 50 times stronger than all other phonons. For yellow or red excitation, it is about as strong as the O(2) E_g and Nd A_{1g} modes, and four times stronger than the O(2) B_{1g} modes. It has been mentioned above that the Nd A_{1g} xx component is at least 10 times weaker than the zz component. The A_{1g}^* xx component is weaker, but shows the same resonance behavior as the zz component. In the blue, also the xx spectra exhibit a rather sharp, well-defined A_{1g}^* peak similar to that in zz polarization. Band-structure calculations[30] showed that below 3 eV only Cu-O transitions are possible (only the antibonding Cu $d_{x^2-y^2}$–$O_{p_{x,y}}$ band is, as usual, crossing E_F), leading as in $YBa_2Cu_3O_7$ (Ref. 29) to weak resonances as observed for the three regular Raman phonons. According to Ref. 30, transitions to Nd bands could occur above 3 eV and would probably lead to an enhancement of the Nd A_g phonon different from the behavior that we observe in our energy range. Thus, the strong A_{1g}^* mode resonance above 2.7 eV indicates that the corresponding electronic transition might not be intrinsic to the proper T' structure. Clearly, more theoretical work on the electronic polarizability and RRS in $Nd_{2-x}Ce_xCuO_4$ is necessary to understand our spectra.

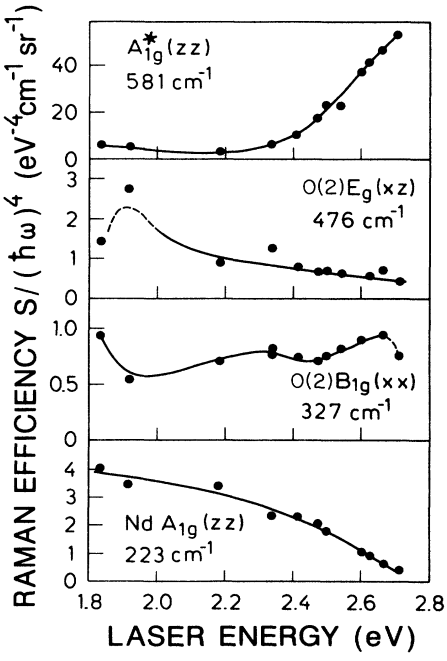

FIG. 10. Resonant Raman efficiencies in absolute units at 295 K for the three Raman-allowed and the strong additional modes in zz (Nd A_{1g}), xx [O(2) B_{1g}], and xz [O(2) E_g], and zz (A_{1g}^*) polarizations, respectively.

The Nd A_{1g} mode resonance profile is substantially altered if no Ce doping is present (no figure). The intensity is then roughly constant, with maxima near 1.9 and 2.5 eV and a minimum at 2.3 eV.

Without showing further figures, we mention some observations concerning Raman intensities: First, the A_{1g}^* intensity increases in Nd-2:1:4 and Sm-2:1:4 by a factor of 3 when the sample is cooled to 10 K, while it stays almost constant for Pr-2:1:4. Second, for Sm-2:1:4 and Pr-2:1:4 the resonance behavior of the A_{1g}^* mode is reversed; it is now strongly resonant in the red (although, in the order of atomic radii, Nd is located between Sm and Pr). This observation points towards an unconventional mechanism for the high Raman intensity of the A_{1g}^* mode.

VI. THE A_{1g}^* MODE NEAR 580 cm^{-1}

Before we discuss the origin of this mode, we summarize our observations concerning it.

(1) It shows clearly A_{1g} selection rules, with a dominating zz component hinting at (but not conclusively proving) a vibration in the z direction.

(2) Its zz component shows a rather sharp peak with a broadened low-energy side; the xx-component is always very broad. The zz peak coincides with the high-energy edge of the xx component. Only in the case of blue resonance the feature exhibits also in xx polarization a sharp peak as in zz configuration. These facts indicate that we are not dealing with a sharp phonon but rather with a density of states between 400 cm^{-1} and a high-frequency cutoff near 590 cm^{-1}.

This observation reminds us of the behavior of amorphous GeO_2,[31] where the totally symmetric Raman configuration yields a sharp peak at 420 cm^{-1}, at the edge of the one-phonon density of states (DOS), while the depolarized Raman scattering is approximately proportional to the DOS. In Refs. 31 and 32, this was explained by a different degree of correlation between the vibrations in various GeO_2 units for totally symmetric and lower-

symmetry vibrations, respectively.

(3) It appears for Nd-2:1:4 only in Ce-doped samples and was also observed in Ce- or Th-doped Sm-2:1:4, Gd-2:1:4, and Pr-2:1:4. Sugai, Kobayashi, and Akimitsu[12] also report it in Ce-free Pr-2:1:4. Thus it does not seem to be merely induced by Ce doping but rather by a somewhat more general structural property of T' R-2:1:4.

(4) Its dependence on rare-earth and temperature (Figs. 5 and 7) is regular, indicating that vibrations of O(2) at its T'-structure position do not contribute substantially to its origin (see Secs. II and III).

(5) In Nd-2:1:4 it is strongly resonant in the blue while for doped Sm-2:1:4 and Pr-2:1:4 it is enhanced for red excitation. But it is very strong even out of resonance.

Its early assignment by us[9] and Orera *et al.*[11] to the highest infrared-active A_{2u} vibration, corresponding to a motion of O(2) against O(1), Raman-activated in some way, cannot be upheld since we have shown that the A_{2u}-LO phonon has an energy of only 559 cm^{-1}.[10] We also know from lattice-dynamical calculations[15] that these highest-frequency modes are essentially dispersionless [A_{2u}, also E_u(LO)=593 cm^{-1}] or decrease in energy when going to the zone edge [E_u(TO)]. Hence, no z-directed vibration has such a high energy.

According to our experience with other materials it seems that a z-direction stretching of a short bond is necessary to warrant a highly zz-polarized peak. We mention here that we found in our z-polarized infrared reflection spectra[10] a peak at 590 cm^{-1} which we attributed to a screening leakage from the highest E_u mode. Since all other E_u phonons were perfectly screened out in these measurements, we now conjecture that this feature might have the same origin as the A_{1g}^* Raman peak.

We first point out that this peak cannot be due to electronic Raman scattering: Ce^{4+} has no f electrons and Ce^{3+} has its lowest transition from the $^2F_{5/2}$ to the $^2F_{7/2}$ state at 2253 cm^{-1},[33] i.e., far too large. Crystal-field splittings of the ground state, however, should not be large enough to account for the 580-cm^{-1} peak.[33] Finally, it cannot be caused by rare earth transitions since it would vary drastically for the different rare earths.

A possible explanation of the origin of this peak that seems to be in agreement with (1)–(5), requires the assumption that some of the O(2) atoms leave their proper T'-structure position and rather settle at the T-structure position closely above or below the rare earth (thus generating T^*-like cells). If considered as a local R-O molecule, the z-directed vibration of this oxygen atom would lead to A_1-symmetry Raman scattering with a dominating zz component. Since we showed in Secs. II and III that Pr-2:1:4 is already close to the transition to T structure, we expect this mode to be particularly strong for Pr-2:1:4. This is indeed the case: The peak is even observed in undoped Pr-2:1:4,[12] and the relative size of this peak with respect to the other phonons seems to be largest in R=Pr (Fig. 2). If we assume that O(2) goes to the T-structure site particularly in the neighborhood of Ce atoms, we can also explain the Ce dependence. The next question is the origin of the DOS observed in xx configuration out of resonance and in zz polarization as the low-energy tail of the 580-cm^{-1} peak. It cannot be induced by the not fully symmetric motion of the displaced O(2) atoms, as mentioned above for amorphous GeO_2,[31] since this would lead to $y(xz)\bar{y}$ intensity. However, the whole feature has clearly "A_{1g}" polarization properties.[9–11] Thus, we probably need another displacement-induced A_{1g} mode that is more strongly dispersive than the first one and yields both xx and zz intensity. The different widths of the two features could also be explained, as demonstrated for amorphous GeO_2 in Ref. 32, by a different degree of correlation between the atomic motion on the various O(2) sites in the partially disordered solid.

In our model as well as for any other model, the crucial question is why this vibrations leads to such high intensities, i.e., bond polarizabilities, even if only some of the O(2) atoms go to the T-structure position. A possible answer might be based on the large polarizabilities that O^{2-} ions can reach if they have more space than usual.[34] This effect is well known to be important for ferroelectric phase transitions.[34] In our case, the p_x or p_y orbitals of the displaced O(2) atoms could reach out very far towards the direction where O(2) would be located in the perfect T' structure.

We consider, however, the assignment at the A_{1g}^* peak to be still an unsettled question. The next step should be a more precise determination of the structure of R-2:1:4 which, to our knowledge, has not been achieved so far. We just mention here that it will not be easy to find "a few" O(2) atoms with neutron scattering, and probably impossible with x-ray diffraction. Raman studies of T^*-structure materials may also be of help.

VII. SUMMARY

In this paper we demonstrate the consequences of structural properties on the Raman spectra of the T'-structure materials. Starting with the structural observation that in Nd-2:1:4 and Pr-2:1:4 the rare-earth–O(2) bonds are strongly under compression, so that the system is close to a transition to the T structure, we find that as a precursor of this transition the O(2) phonons are anomalously soft for R=Pr. In parallel with this softening goes an increase of anharmonicity leading to strongly negative and positive temperature dependences of the B_{1g} phonon frequencies.

From studying the dependence on doping we conclude that the E_g mode is strongly affected by the changes in the electronic structure and can thus be used to characterize the Ce content. We then presented the resonance behavior of the Raman modes, which might, with the help of band-structure calculations as in Ref. 30, lead to a better understanding of the electronic structure.

The last part of this paper dealt with those modes induced by deviations from the perfect tetragonal lattice such as superlattices, vacancies, or partial $T \leftrightarrow T'$ transitions by some of the O(2) atoms. The first groups seem to

be responsible for several peaks observed in $z(x*)\bar{z}$ configuration in undoped Nd_2CuO_4, while the latter might cause the prominent zz-polarized feature near 590 cm^{-1}.

ACKNOWLEDGMENTS

We would like to thank W. Kress for stimulating discussions concerning the lattice dynamics, C. Thomsen for a critical reading of the manuscript, R. Kremer for measuring the magnetic susceptibility, and K. Peters for x-ray analyses. Thanks are also due to H. Hirt, M. Siemers, and P. Wurster for expert technical help. We gratefully acknowledge financial support from the Bundesminister für Forschung und Technologie and the European Community.

---

*Permanent address: Department of Physics, Materials Research Laboratory, University of Illinois at Urbana-Champaign, 104 S. Goodwin Ave., Urbana, IL 61801.

†Permanent address: Institut Ciència de Materials de Barcelona, Barcelona, Spain.

[1] J.G. Bednorz and K.A. Müller, Z. Physik B **64**, 189 (1986).

[2] Y. Tokura, H. Takagi, and S. Uchida, Nature **337**, 334 (1989).

[3] J.T. Markert and M.B. Maple, Solid State Commun. **70**, 145 (1989).

[4] B. Grande, Hk. Müller-Buschbaum, and M. Schweizer, Z. Anorg. Allg. Chem. **428**, 120 (1977).

[5] Y.Y. Xue, P.H. Hor, R.L. Meng, Y.K. Tao, Y.Y. Sun, Z.J. Huang, L. Gao, and C.W. Chu, Physica C **165**, 357 (1990).

[6] R.D. Shannon and C.T. Prewitt, Acta Crystallogr. B **25**, 925 (1969).

[7] S. Sugai, T. Kobayashi, and J. Akimitsu, Phys. Rev. B **40**, 2686 (1989).

[8] V.G. Hadjiev, J.Z. Kostadinov, L. Bozukov, E. Dinolova, and D.M. Mateev, Solid State Commun. **71**, 1093 (1989).

[9] E.T. Heyen, R. Liu, B. Gegenheimer, C. Thomsen, M. Cardona, S. Piñol, and D.McK. Paul, in *PHONONS '90*, edited by S. Hunklinger, W. Ludwig, and G. Weiss (World Scientific, Singapore, 1990), p. 346.

[10] E.T. Heyen, G. Kliche, W. Kress, W. König, M. Cardona, E. Rampf, J. Prade, U. Schröder, A.D. Kulkarni, F.W. de Wette, S. Piñol, D.McK. Paul, E. Morán , and M.A. Alario-Franco, Solid State Commun. **74**, 1299 (1990).

[11] V.M. Orera, M.L. Sanjuán, R. Alcalá, J. Fontcuberta, and S. Piñol, Physica C **168**, 161 (1990).

[12] S. Sugai, T. Kobayashi, and J. Akimitsu, Solid State Commun. **74**, 599 (1990).

[13] M.K. Crawford, G. Burns, G.V. Chandrashekhar, F.H. Dacol, W.E. Farneth, E.M. McCarron III, and R.J. Smalley, Solid State Commun. **73**, 507 (1990).

[14] M.K. Crawford, G. Burns, G.V. Chandrashekhar, F.H. Dacol, W.E. Farneth, E.M. McCarron III, and R.J. Smalley, Phys. Rev. B **41**, 8933 (1990).

[15] W. Kress *et al.* (unpublished).

[16] E. Morán, A.I. Nazzal, T.C. Huang, and J.B. Torrance, Physica C **160**, 30 (1989).

[17] S. Piñol, J. Fontcuberta, C. Miravitlles, and D. McK. Paul, Physica C **165**, 265 (1990).

[18] *Powder diffraction file* (International Center for Diffraction Data, Swarthmore, 1988).

[19] M.J. Rosseinsky, K. Prassides, and P. Day, Physica C **161**, 21 (1989).

[20] G.H. Kwei, S.-W. Cheong, Z. Fisk, F.H. Garzon, J.A. Goldstone, and J.D. Thompson, Phys. Rev. B **40**, 9370 (1989).

[21] For example, the 465-cm^{-1} mode in $Bi_2Sr_2CaCu_2O_8$, see G. Burns, G.V. Chandrashekhar, F.H. Dacol, and P. Strobel, Phys. Rev. B **39**, 775 (1989).

[22] A.A. Abrikosov, L.P. Bor'kov, and I.E. Dzyaloshinski, *Methods of Quantum Field Theory in Statistical Physics* (Prentice-Hall, New Jersey, 1963).

[23] J.M. Tarascon, E. Wang, L.H. Greene, B.G. Bagley, G.W. Hull, S.M. D'Egidio, P.F. Miceli, Z.Z. Wang, T.W. Jing, J. Clayhold, D. Brawner, and N.P. Ong, Phys. Rev. B **40**, 4494 (1989).

[24] P. Lightfoot, D.R. Richards, B. Dabrowski, D.G. Hinks, S. Pei, D.T. Marx, A.W. Mitchell, Y. Zheng, and J.D. Jorgensen, Physica C **168**, 627 (1990).

[25] R.E. Cohen, W.E. Pickett, and H. Krakauer, Phys. Rev. Lett. **62**, 831 (1989).

[26] C.H. Chen, D.J. Werder, A.C.W.P. James, D.W. Murphy, S. Zahurak, R.M. Fleming, B. Batlogg, and L.F. Schneemeyer, Physica C **160**, 375 (1989).

[27] T. Williams, Y. Maeno, J. Mangelschots, A. Reller, and G. Bednorz, Physica C **161**, 331 (1989).

[28] M. Cardona, in *Light Scattering in Solids II*, edited by M. Cardona and G. Güntherodt (Springer, Heidelberg, 1982).

[29] E.T. Heyen, S.N. Rashkeev, I.I. Mazin, O.K. Andersen, R. Liu, M. Cardona, and O. Jepsen, Phys. Rev. Lett. **65**, 3048 (1990).

[30] K. Takegahara and T. Kasuya, Solid State Commun. **70**, 637 (1989).

[31] R.M. Martin and F.L. Galeener, Phys. Rev. B **23**, 3071 (1981).

[32] P.N. Sen and M.F. Thorpe, Phys. Rev. B **15**, 4030 (1977).

[33] G.H. Dieke, in *Spectra and Energy Levels of Rare Earth Ions in Crystals*, edited by H.M. Crosswhite and H. Crosswhite (Interscience, New York, 1968).

[34] A. Bussmann, H. Bilz, R. Roenspiess, and K. Schwarz, Ferroelectrics **25**, 343 (1980).